HEALTH SYSTEMS
2024, VOL. 13, NO. 1, 62–72
https://doi.org/10.1080/20476965.2022.2125838

THE OPERATIONAL RESEARCH SOCIETY
Taylor & Francis
Taylor & Francis Group

RESEARCH ARTICLE

Vision-based gait analysis for real-time Parkinson disease identification and diagnosis system

Sathya Bama B[a] and Bevish Jinila Y[b]

[a]Computer Science and Engineering, Sathyabama Institute of Science and Technology, Chennai, India; [b]Sathyabama Institute of Science and Technology, Chennai, India

ABSTRACT

Computer-assisted Parkinson's disease-specific gait pattern recognition has gained more attention in the past decade due to its extensive application. In this research study, vision-based gait feature extraction is obtained from the observed skeleton points to support the real-time Parkinson disease prediction and diagnosis in the smart healthcare environment. So, a novel kernel-based principal component analysis (KPCA) is introduced for establishing respective feature extraction and dimensionality reduction on the patient's video data. In this research study, a vision-based Parkinson disease identification system (VPDIS) is developed with a feature-weighted minimum distance classifier model to support the clinical assessment of Parkinson's disease. At the time of experimentation, a steady-state walking style of the patient was captured using the cameras fixed in the smart healthcare environment. Then, the accumulated walking frames from the remote patients were transformed into the required binary silhouettes for the sake of noise minimisation and compression purpose. The resulting experimentation shows that the proposed feature extraction approach has significant improvements on the recognition of target gait patterns from the video-based gait analysis of Parkinson's and normal patients. Accordingly, the proposed VPDIS using feature-weighted minimum distance classifier model provides better prediction time and classification accuracy against the existing healthcare systems that is developed using support vector machine and ensemble learning classifier models.

ARTICLE HISTORY
Received 25 April 2021
Accepted 8 September 2022

KEYWORDS
Parkinson prediction; vision-based gait analysis; feature extraction; machine learning; distance classifier; healthcare system

1. Introduction

Parkinson's disease is identified as the incurable and most severe neurodegenerative disease that may affect daily living activities (Kruger et al., 2017). However, there is some mechanism to provide a slight control over the motor and non-motor symptoms of Parkinson's patients. At present, very few motor symptoms exist such as tremors, bradykinesia, and postural instability. But there are many non-motor symptoms that exist such as dementia, depression, low pressure, digestion issue, leg discomfort, stability sense, temperature compassion, dysautonomia, akinesia, loss of synchronisation, and so on (Mamun et al., 2017). In past two decades, many researchers showed their focus mainly on non-motor symptoms such as depression, pain, sweating, nervousness, vision, and weight loss. Moreover, much research focus is not given by the biomarkers for developing Parkinson's disease prediction and diagnosis based on clinical assessment of those symptoms. Most of the Parkinson-affected patients are above the age of 65 and live alone in the home (Vermilyea & Emborg, 2018). The primary goal of the caregiver is to improve the long-term prediction of disease by minimising its impact on the daily living activities of the patient. In addition to theoretical knowledge, more practical knowledge and experience might be required regarding Parkinson's disease for doing the caregiver duty. Owing to this situation, the pressure on the caregiver will increase as the disease progresses day by day (Hellqvist & Berterö, 2015). Therefore, an online specialist is required to assess the variation in medical diagnosis and also assess the feedbacks of patients in terms of effects and side effects. Accordingly, the specialist can easily identify the best healthcare professionals such as physiotherapists and speech therapists to take care of the patients. To overcome these problems, the proposed research study plans to incorporate the onboard assessment methodology for the remote healthcare system.

An analytic hierarchy process is enforced in the existing study to assess the tele-healthcare systems involved in Parkinson's disease management and monitoring activities. This framework could help the decision-making process of various stakeholders during the exploitation of new technologies in handling Parkinson's disease (Cancela et al., 2015). To support this type of remote monitoring activities, all the patients need to be connected with medical equipment using an enormous number of cables. So,

CONTACT Sathya Bama B sathyabama9392@gmail.com Computer Science and Engineering, Sathyabama Institute of Science and Technology, Chennai 600119, India

a wireless body area network technology consisting of various wireless sensor nodes and mobile devices is implemented in the remote healthcare system to facilitate the autonomy and mobility of the patients (Kim & Lee, 2014). Further improvement is made to enhance the efficiency and cost-effectiveness of the healthcare system by incorporating the people-centric sensing framework. It provides uninterruptable real-time medical services and emergency care to virtual patients. Therefore, this framework is more suitable for the emerging environment involving large-scale, opportunistic, and mobile application areas (Hussain et al., 2015). A cloud-based secure and dominant storage infrastructure is preferred to minimise the energy consumption and query processing latency among the healthcare systems. This could substantially improve the real-time data sensing and diagnosis of remote patients by minimising both communication and processing costs (Diallo et al., 2014). Most of the research studies do not give much emphasis on improving the prediction time and accuracy of Parkinson recognition systems. These factors motivate the proposed research study towards the improvement of prediction time and accuracy using the appropriate feature extraction and prediction approaches.

A key contribution of this research study includes: (a) the design and development of VPDIS in the cloud; computing platform by improving the data sensing and diagnosis of remote patients; (b) novel KPCA feature extraction technique is enforced to improve the robustness of disease prediction and diagnosis by reducing the dimensionality of patient data; and (c) a feature-weighted minimum distance classifier model is developed to effectively classify the Parkinson persons from the normal persons. The rest of the research study is structured as follows: The next section will give a detailed description of various cloud-based healthcare systems development pertaining to Parkinson disease prediction and diagnosis. In section 3, the complete architecture of VPDIS is explained with the formulation of a vision-based gait pattern recognition problem. Moreover, the proposed KPCA feature extraction technique is discussed along with the proposed feature-weighted minimum distance classifier model to support real-time disease prediction and diagnosis. Section 4 furnishes the complete description of experimental settings and datasets for making a comparative analysis of various healthcare systems. The final section endows with conclusions and future enhancements of this research study.

1. Related works

The Parkinson disease symptom is basically classified into motor and non-motor symptoms. Accordingly, the computer-based Parkinson disease diagnosis system was developed in the context of speech processing, facial expression, handwriting recognition, sensor, and vision-based gait analysis. A speech articulation kinematics is defined to identify the difference between Parkinson's and normal patients according to time domain-based speech features (Gómeza et al., 2019). To best suit the real-time prediction and diagnosis of Parkinson's, speech impairments are analysed with the help of the Hilbert spectrum-based feature selection method (Karan et al., 2020). Similarly, acoustic features of a patient's voice samples are extracted in the cepstral domain using two effective methods such as Mel-frequency cepstral coefficients and perceptual linear prediction, respectively (Benmalek et al., 2018). Next, a cognitive impairment-based facial expression recognition is implemented with visual exploration using the analysis of various eye movement behaviours (Waldthaler et al., 2019). Since the evaluation of a facial expression is more time-consuming, the computational analysis technique was explored to assist the specialist during the clinical decision-making on patients affected by Parkinson's disease or not (Sonawane & Sharma, 2021). Euclidean distance-based facial expressions are analysed in the vision-based systems to clearly quantify the changes occurring in the facial expressivity and movements for the appropriate prediction and rehabilitation process (Bandini et al., 2017). Early identification of Parkinson's disease was assessed using the enforcement of deep transfer learning on the patient handwriting dynamics. Due to neural changes, patients have major problems in controlling the movement of the body and motor-based works (Kamran et al., 2021). One of the most typical symptoms of Parkinson's disease is micrographia which can be recognised using computer-aided handwriting dynamics. So, an ensemble learning model is introduced with the combination of principal component analysis and random forest classifier models (Xu & Pan, 2020). Efficient feature selection from the handwriting datasets is considered to be the key challenging problem.

Wrist-worn accelerometer sensors were used to monitor the motor symptoms of Parkinson's patients (Fisher et al., 2016). To recognise the patient activity, the time, frequency, and statistical domain features are extracted from the three-dimensional accelerometer sensors deployed on the human body (Machado et al., 2015). A support vector machine-based postural detection approach was used to recognise the various daily living activities of Parkinson's patients during the real-time monitoring and assessment of postural transitions (Rodriguez-Martin et al., 2013). Therefore, the multi-sensor-based gait analysis helps to recognise the behaviour of the neural system at the time of early prediction and diagnosis of Parkinson's disease (Nancy Noella et al., 2019). Under sensor-based gait

analysis, effective feature selection and classification approaches become the challenging task to reduce the computation time and improve the prediction accuracy. In the vision-based gait analysis, a novel low-cost vision system was introduced based on machine-learning approaches to recognise Parkinson's disease and its severity stages automatically (Buongiorno et al., 2019). Similarly, a vision-based gait destruction analysis was made using the gait and posture-based features extraction to quantify the gait impairment and fall risk of patients (Ortells et al., 2018). Identifying the sensitivity of feature selection and providing accurate motion data without affecting the motion pattern and gait perception from the vision system is identified as key research issues in the healthcare systems. Therefore, the proposed research study focused on developing a VPDIS using the KPCA- and LDA-based feature extraction techniques to resolve the vision-based gait pattern recognition problems.

To predict the severity level of Parkinson patient fall, a novel postural stability indicator was developed to overcome the issues like independent risk factor and fear of falling measurements. These measurement helps the clinicians to correctly identify the postural stability of the patients that helps to make the effective analysis on centre of pressure and postural control performance measures (Pourghayoomi et al., 2020). In the aspects of clinical evaluation, the demographic data, disease related data, suppositories, and the presence of response fluctuations were used to identify the different types of diseases such as tremor predominant, and akinetic rigid (Khlebtovsky et al., 2017). Another aspect of objective poster evaluation was made using the hand-held device to identify the spinal mobility, and range of motion by adjusting the contour of the spine with respect to three different positions. In the next level, osteoporosis and physical activity evaluation are considered to be the most standard measurement for the diagnosis. Postural deformities are identified as a severe impact of Parkinson's progression that leads to severe flexion of spine during the time of walking and standing positions (Debû et al., 2018). These types of measurement and prediction systems are used for managing gait and posture in Parkinson disease.

2. Architecture of VPDIS

The layered architecture of the proposed VIPDIS is represented in Figure 1. It consists of a vision-based sensor and cloud computing layers for real-time patient data sensing and its disease predictions, respectively. In the vision-based sensor layer, the raspberry pi-3 device is embedded with a camera module to lively capture the human motion that can be used to recognise the Parkinson's disease gait patterns. The raspberry pi-3 device will dynamically supply the vision-based data to the proposed classifier model deployed in the cloud computing layer. As a result, the feature-weighted minimum distance classifier model could apply the decision rule by computing the minimum distance metric among the patient's data mapped in the medical history. Then, the final decision of the classifier will give the accurate classification of Parkinson's disease persons from the normal persons. Based on the severity stages of disease, the telemedicine suggestions and prescriptions are given to the concern by online experts readily available in the healthcare system. The motivation behind the Parkinson's severity stage identification is to keep track of Parkinson's disease progression after diagnosis and treatments. This will help to take preventive care before getting a worsening symptoms and fluctuations that may lead to the prediction of human falls and other imbalance body movements of patient. Here, the proposed VIPDIS have the varied healthcare implications that can help the caretakers/nurses to keep track of changes happening in the healthcare systems by offering needful service delivery to the elderly or remote patients. In this connection, online experts available in the proposed healthcare system will suggest the latest therapies such as medications and deep brain simulations to the patients. Moreover, the proposed VIPDIS consists of various cloud-based interconnected elements such as patient medical history database, disease prediction classifier, and rehabilitation monitoring and assessment services deployed in the cloud layer works along with devices like Raspberry Pi-3 and smart phone deployed in the vision-based sensor layer. In this healthcare system, progression of Parkinson's disease symptoms can be closely measured in terms of severity stages. Then, the healthcare system will suggest the appropriate disability requiring therapy based on the severity stages during the rehabilitation monitoring and assessment process. To identify the deviations in the patient's health status, continuous assessment and monitoring are done during the rehabilitation process. Consequently, the health status indication is given to the concerned patient's mobile phone through a healthcare monitoring application. The formulation of vision-based gait pattern recognition, feature extraction, and disease prediction classifier model is given in the subsequent subsections.

2.1. Formulation of vision-based gait recognition problem

Vision-based gait analysis provides an investigative feature extraction from the silhouettes of a person walking motion captured using the smart cameras. So, a novel gait pattern recognition approach is required for identifying the variations of walking

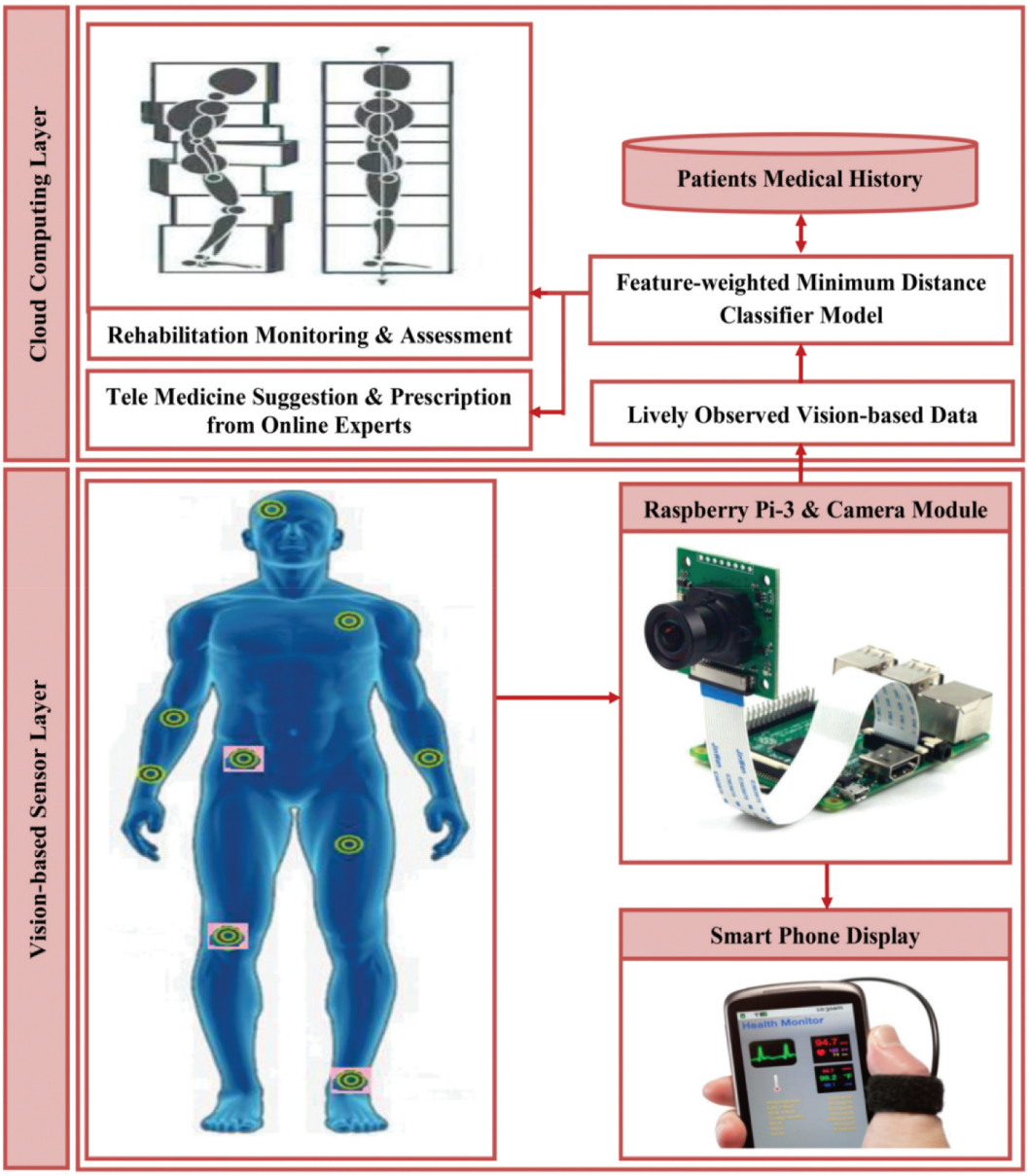

Figure 1. Layered architecture of VPDIS.

states and poses acquired from the end-user camera. To represent the human gait, the proposed study explores the covariance among the skeletal joints merged with their respective trajectory positions and speed to model the corresponding movements. In addition, the joint transformation of the motion sequence will suffer from patients walking cycle position and speed normalisation problems. To overcome such problems, the sequence of motion is segmented into several fixed-size local windows and wounding the motion frames along the timeline that could permit the invariance in walking cycle and speed without any kind of synchronisation mechanism. Leaning the similarity distance among the trained gait models helps in improving the accuracy rate of gait classification. The classification requires only the patient's walking patterns from the observed silhouette data rather than the background scenes. A sequence of motion-captured during the time period $\tau \in [1, 2, \ldots, T]$ consists of a set of skeletons defined by 25 joints. The i^{th} joint representation at any time τ can be expressed by Equation (1).

$$\rho_i^\tau = \begin{bmatrix} x_i^\tau \\ y_i^\tau \\ z_i^\tau \end{bmatrix} \tag{1}$$

The size of the skeleton will gradually increase when the patient moves towards the camera. To achieve the scale-invariant skeleton, the Euclidean distance is fixed between the shoulder-centre and hip-centre during the patient walks. As a result, the skeleton joints are normalised with respect to their distance from the hip-centre $\rho_i^\tau - \rho_{HC}^\tau$. Also, the skeleton can

be rotated towards the global orientation based on vector connecting both the hips with respect to the global X-axis.

To acquire the invariance of complete body positions, a local relative coordinate mechanism is explored to characterise the skeletal joints. So, select the hip centre joint as the source of local coordinate and symbolise the remaining skeletal joints to yield the normalised coordinates per frame as denoted by Equation (2).

$$\bar{\mathcal{P}}^{\tau} = \begin{bmatrix} x_1^{\tau}, x_2^{\tau} \ldots, x_{24}^{\tau} \\ y_1^{\tau}, y_2^{\tau}, \ldots, y_{24}^{\tau} \\ z_1^{\tau}, z_2^{\tau}, \ldots, z_{24}^{\tau} \end{bmatrix} \tag{2}$$

where $\bar{\mathcal{P}}$ be the skeletal joints positions. Then, the corresponding positional covariance matrix is measured along the motion trajectories as defined by Equation (3).

$$Cov\left(\bar{\mathcal{P}}\right) = \frac{1}{N-1}\sum_{\tau=1}^{T}\left(\bar{\mathcal{P}}^{\tau} - \mu\right)\left(\bar{\mathcal{P}}^{\tau} - \mu\right)^{T} \tag{3}$$

where μ be the mean value of $\bar{\mathcal{P}}$, $N = 24$ be the normalised skeletal joints, and $\bar{\mathcal{P}}\tau$ be the 3×24 dimensional feature point observation made at time period $\tau \in [1, T]$. Such covariance estimation could provide only the common joint positions available along the time frame to effectively recognise the gait containing a strong spatial difference such as running, walking, raising hands, and so on. In case of motion observed from Parkinson's affected patients contain similar joint trajectory patterns show very less spatial variance. Therefore, the classification of the spatial pattern of motion becomes more challenging and insufficient for the healthcare systems to make appropriate predictions under complex patterns and motion deficiency. As a result, the motion representation is enhanced with the relative speed of joints to estimate the covariance matrix as given by Equation (4). Then, the corresponding gradient set of joints are defined by Equation (5).

$$Cov(\mathcal{G}) = \frac{1}{N-1}\sum_{\tau=1}^{T}(\mathcal{G}^{\tau} - \hat{\mu})(\mathcal{G}^{\tau} - \hat{\mu})^{T} \tag{4}$$

$$\mathcal{G}_i^{\tau} = \begin{bmatrix} x_i^{\tau} - x_i^{\tau-1} \\ y_i^{\tau} - y_i^{\tau-1} \\ z_i^{\tau} - z_i^{\tau-1} \end{bmatrix} \tag{5}$$

Let $\mathcal{G}^{\tau}$ be the twenty-four-dimensional point observed at time period τ and $\hat{\mu}$ be the mean value of $\mathcal{G}^{\tau}$.

The matrix distance function is introduced to find the dissimilarity between any two covariance matrices as defined by Equation (6).

$$d(Cov(p), Cov(q)) = \sqrt{\sum_{i=1}^{n} ln^2 \lambda_i(Cov(p), Cov(q))} \tag{6}$$

where ln^2 denotes the natural logarithm and $\lambda_i(\cdot)$ be the widespread Eigen values of $Cov(p)$ and $Cov(q)$ with the intention of satisfying the condition $Cov(p)x = \lambda Cov(q)x$. Here, the variable x denotes the generalised right Eigen vector. Based on the matrix distance metric, the covariance value can be used to learn the distinctive classifier. Therefore, the dissimilarity measurement satisfies all the conditions given in Equation (7).

$$\begin{cases} d(Cov(p), Cov(q)) \geq 0 \\ d(Cov(p), Cov(q)) = 0 \end{cases} \begin{bmatrix} iff Cov(p) = Cov(q), \\ d(Cov(p), Cov(q)) = d(Cov(q), Cov(p)), and \\ d(Cov(p), Cov(q)) + d(Cov(q), Cov(r)) \geq d(Cov(p), Cov(r)) \end{bmatrix} \tag{7}$$

After the formulation of covariance matrix distance, a term frequency-based inverse document frequency approach is explored by the supervised learning classifier model. For the given training window, the term frequency in class C can be expressed by Equation (8) with the concatenation of positional ρ and speed $\mathcal{G}$ matrices.

$$\mathcal{TF}\left(\mathcal{W}_I^C\right) = \sum_{i=1}^{\left|\mathcal{W}^C\right|} \frac{Sim\left(\mathcal{W}_I^C, \mathcal{W}_J^C\right)}{\left|\mathcal{W}^C\right|} \tag{8}$$

Let $\left|\mathcal{W}^C\right|$ denote the number of windows present in class C, and the $Sim(\cdot)$ function gives the binary distance between the covariance matrices of windows as defined by Equation (9).

$$Sim\left(\mathcal{W}_I^C, \mathcal{W}_J^C\right) = \begin{cases} 1, if d\left(Cov\left(\mathcal{W}_I^C\right), Cov\left(\mathcal{W}_J^C\right)\right) < \varepsilon \\ 0, \qquad\qquad Otherwise \end{cases} \tag{9}$$

Afterwards, the window distinctiveness can be estimated based on the inverse frequency of its look in another class by the calculation of the quantity of occurrence of $\mathcal{W}_I^C$ in all classes as stated by Equation (10). Here, the occurrence of $\mathcal{W}_I^C$ is defined by Equation (11).

$$\mathcal{IDF}\left(\mathcal{W}_I^C\right) = \log\frac{|c|}{\sum_j^{|c|} Occ\left(\mathcal{W}_I^C, j\right)} \tag{10}$$

$$Occ\left(\mathcal{W}_I^C, j\right) = \begin{cases} 1, if \sum^{\left|\mathcal{W}^j\right|} Sim\left(\mathcal{W}_I^C, \mathcal{W}_K^C\right) > 0 \\ 0, \qquad\qquad Otherwise \end{cases} \tag{11}$$

The classification performance is learned from all the windows available from the training set based on the distinctiveness measured with respect to the class C in terms of weight factor expressed by Equation (12).

$$Weight\left(\mathcal{W}_I^C\right) = \mathcal{TF}\left(\mathcal{W}_I^C\right) \times \mathcal{IDF}\left(\mathcal{W}_I^C\right) \tag{12}$$

During the vision-based gait pattern classification, the motion sequence S is first segmented into h number of frames denoting the fixed-size time window. Afterwards, compute the positional and speed covariance matrices of joints present in each time window. To compute the k-closest nearest neighbours of the training sequence, the matrix similarity function $d(\cdot)$ is explored during experimentation. Accordingly, the k-nearest neighbours obtained with respect to the testing sequence $\mathcal{W}_I^* \in S$ of unknown class $(*)$ is given as $k\_Closest(\mathcal{W}_I^*)$. Then, the classification is done per each class C can be measured using average weighted distance of $\mathcal{W}_I^*$ to its k-nearest neighbours in C as formulated by Equation (13).

$$\mathcal{W}\_Distance(\mathcal{W}_I^*, C) = \sum_{\mathcal{W}_{\mathcal{P}}^C \in k\_Closest(\mathcal{W}_I^*)} \frac{Weight(\mathcal{W}_I^C) \cdot d(Cov(\mathcal{W}_I^C), Cov(\mathcal{W}_{\mathcal{P}}^C))}{|\mathcal{W}_{\mathcal{P}}^C|} \tag{13}$$

Let $|\mathcal{W}_{\mathcal{P}}^C|$ denote the number of windows present in the k-nearest neighbours set of $\mathcal{W}_I^*$ of class C. Lastly, compute the class similarity among the S and C denoting the average weighted distance of their windows as shown by Equation (14).

$$Class\_Sim(S, C) = \frac{1}{|\mathcal{W}_I^* \in S|} \sum_{\mathcal{W}_I^* \in S} \mathcal{W}\_Distance(\mathcal{W}_I^*, C) \tag{14}$$

Since the research study focuses on silhouette data of patient walking sequence, the background images of gait sequence can be discarded during gait analysis. Therefore, the brightness intensity of the respective background image pixel construction is done based on the intensity median value present on each pixel located in the entire gait sequence as defined by Equation (15).

$$\mathcal{B}(i,j) = \mathcal{IM}_{total}(I_\tau(i,j)) \tag{15}$$

where $\mathcal{IM}_{total}$ denotes the intensity median observed among the total images available in the complete gait sequence, $I_\tau(i,j)$ denotes the brightness observed on the image at position (i,j) that communicate during the time period τ. To acquire the silhouette pixel containing various walking patterns of patients can be estimated through the difference method shown in Equation (16). Next, the threshold value ϕ is determined to separate the walking silhouette from the corresponding sequential image frames as formulated by Equation (17). Accordingly, the brightness value of the silhouette pixel can be initialised as given in Equation (18).

$$\mathcal{P}_\tau(i,j) = 1 - \frac{2 \times \sqrt{(I_\tau(i,j)+1)(\mathcal{B}(i,j)+1)}}{(I_\tau(i,j)+1)+(\mathcal{B}(i,j)+1)} \times \frac{2 \times \sqrt{(256 - I_\tau(i,j))(256 - \mathcal{B}(i,j))}}{(256 - I_\tau(i,j)) + (256 - \mathcal{B}(i,j))} \tag{16}$$

$$\phi = \frac{1}{\mathcal{N}} \sum^{\frac{\mathcal{B}(i,j)}{256}} \tag{17}$$

$$\begin{cases} \mathcal{P}_\tau(i,j) = 1, if \mathcal{P}_\tau(i,j) > \phi \\ \mathcal{P}_\tau(i,j) = 0, if \mathcal{P}_\tau(i,j) < \phi \end{cases} \tag{18}$$

Let $\mathcal{N}$ be the total number of pixel and the threshold value of the respective background image pixel is normalised to the range $[0, 1]$. Then, the binary silhouette image of respective frames is trimmed to identify the walking patterns of Parkinson's patients. Finally, feature extraction and dimensionality reduction approaches are utilised to reduce the computational cost and eliminate the redundancies during the time of foreground object identification by means of counting the pixels.

2.2. Feature extraction and dimensionality reduction using KPCA

The KPCA is introduced to extract the non-linear components and minimise the image noise using kernel methods. This feature extraction approach helps in minimising the dimensionality of input data space by converting higher dimensional into a lower dimensional data space. Consider, there are n number of vectors grouped into c number of classes. These vectors can be represented as $\mathcal{X}_{11}, \ldots, \mathcal{X}_{1n}, \ldots, \mathcal{X}_{i1}, \ldots, \mathcal{X}_{in}, \ldots, \mathcal{X}_{c1}, \ldots, \mathcal{X}_{cn}$, which includes the set of the n-dimensional vector. Here, the variable $\mathcal{X}_{ij}$ denotes the j^{th} vector of i^{th} class, and n denotes the number of vectors in i^{th} class. Then, the mean value of a complete set of vectors is computed by Equation (19).

$$\mu_{\mathcal{X}} = \frac{1}{n} \sum_{i=1}^{c} \sum_{j=1}^{n} \mathcal{X}_{ij} \tag{19}$$

Next, the covariance matrix is measured to investigate the non-linear components (polynomial functions) of $\mathcal{X}$ as defined in Equation (20) by mapping the vectors $\mathcal{X}$ to the feature space $\mathcal{H}$.

$$\mathcal{C} = \frac{1}{n} \sum_{i=1}^{c} \sum_{j=1}^{n} (\mathcal{X}_{ij} - \mu_{\mathcal{X}})(\mathcal{X}_{ij} - \mu_{\mathcal{X}})^T \tag{20}$$

where T encloses the centralised mapped data of the respective transpose matrix. Assume, the variable $\mathcal{K}$ be the rank of $\mathcal{C}$, then the corresponding Eigen values and vectors are formulated as $[\lambda_1, \lambda_2, \ldots, \lambda_{\mathcal{K}}]$ and $[\rho_1, \rho_2, \ldots, \rho_{\mathcal{K}}]$, respectively. In the case without any loss of generality, obtain the constraints as expression as $|\lambda_1| \geq |\lambda_2| \geq \ldots \geq |\lambda_{\mathcal{K}}|$. An incomplete Eigen space could be spitted into an incomplete set of Eigen vectors $k \leq \mathcal{K}$ such as $[\rho_1, \rho_2, \ldots, \rho_k]$. Then, the concluding projection $\mathcal{Y}_{ij}$ of each vector $\mathcal{X}_{ij}$ on the incomplete space can be acquired using Equation (21). Let $\mathcal{Y}_{ij}$ be the PCA coefficient of this research study.

$$\mathcal{Y}_{ij} = \left[\rho_1, \rho_2, \ldots, \rho_k\right]^T \mathcal{X}_{ij} = \boldsymbol{\rho}\mathcal{X}_{ij} \tag{21}$$

Finally, solve the expression given in Equation (22) to acquire the Eigen value and Eigen vector of the covariance matrix $\mathcal{C}$. It is more challenging to resolve the covariance matrix $\mathcal{C}$ due to the infinite dimensionality of the vector $\mathcal{X}_{ij}$.

$$\lambda\mathcal{V} = \mathcal{C}\mathcal{V} \tag{22}$$

As a result, a new centralised kernel matrix $\hat{\mathcal{K}}$ is defined with $n \times n$ dimension to obtain both the Eigen value and vector of the covariance matrix $\mathcal{C}$ as expressed by Equation (23). Afterwards, the kernel function is formulated in terms of vectors as given in Equation (24).

$$\hat{\mathcal{K}} = \left(\mathcal{X}_i - \mu_{\mathcal{X}}\right) \cdot \left(\mathcal{X}_j - \mu_{\mathcal{X}}\right) = \mathcal{K} - l_n\mathcal{K} - \mathcal{K}l_n + l_n\mathcal{K}l \tag{23}$$

$$\mathcal{K}_{ij} = \mathcal{X}_i \cdot \mathcal{X}_j = k\left(\mathcal{X}_i, \mathcal{X}_j\right) \tag{24}$$

where $(l_n)_{ij} = \frac{1}{n}$, and the value of i and j denotes the indices of row and column correspondingly. To acquire the product of vectors from the original space, a polynomial kernel function is defined by Equation (25) with respect to the value of $d > 1$. In the case of PCA the value of $d = 1$, and the proposed KPCA takes the value of $d > 1$.

$$k\left(\mathcal{X}_i, \mathcal{X}_j\right) = \left(\mathcal{X}_i \cdot \mathcal{X}_j\right)^d \tag{25}$$

The relationship between the Eigen vectors $\hat{\mathcal{V}}$ and $\mathcal{V}$ belonging to the corresponding kernel matrix $\hat{\mathcal{K}}$ and covariance matrix $\mathcal{C}$ could be measured using Equation (26).

$$\mathcal{V}_k = \frac{1}{\sqrt{\widehat{\lambda}_k}} Q\widehat{V}_k \tag{26}$$

Let $\widehat{\lambda}_k$ be the nonzero set of values of $\hat{\mathcal{V}}$, $k = 1, 2, \ldots, m$ be the nonzero Eigen values, and Q be the centralised dataset mapping. The sequence of mapping dataset can be defined as given by Equation (27).

$$Q = \left[\left(\mathcal{X}_1 - \mu_{\mathcal{X}}\right)\left(\mathcal{X}_2 - \mu_{\mathcal{X}}\right) \ldots \left(\mathcal{X}_n - \mu_{\mathcal{X}}\right)\right] \tag{27}$$

After the projection of mapping dataset to the feature space created by the vectors $\mathcal{V}_1, \mathcal{V}_2, \ldots, \mathcal{V}_m$, the k^{th} feature vector of required KPCA $\mathcal{Y}_k$ can be formulated by Equation (28).

$$\mathcal{Y}_k = \mathcal{V}_k^T Q = \frac{1}{\sqrt{\widehat{\lambda}_k}} \hat{\mathcal{V}}_k^T Q^T Q = \frac{1}{\sqrt{\widehat{\lambda}_k}} \hat{\mathcal{V}}_k^T \hat{\mathcal{K}} \tag{28}$$

where T denote the transpose matrix. The proposed KPCA helps to minimise the dimensionality of the required image frames with several nonlinear mechanisms. As a result, the proposed approach chooses the key gait pattern mechanisms from the patient walking image sequence.

2.3. Parkinson disease prediction using feature-weighted minimum distance classifier

To classify the Parkinson affected person from the normal person, a minimum distance classifier model is introduced as defined by Equation (29).

$$_{MD} = \arg Min_i \left[\left(\mathcal{Y}_i - m_i\right)^T \left(\mathcal{Y}_i - m_i\right)\right] \tag{29}$$

where T be the data corresponding to the transposed matrix and $\left(\mathcal{Y} - m_i\right)^T \left(\mathcal{Y} - m_i\right)$ be the squared Mahalanob is distance measurement between $\mathcal{Y}$ and m_i. It can be expressed by the squared Euclidean distance as shown in Equation (30).

$$\delta_i^2 = \sum_{i=1}^{d} \left(\mathcal{Y}_i - m_i\right)^2 \tag{30}$$

Let $\mathcal{Y}_i$ be the i^{th} feature and d be the dimension of the feature vector. Consequently, the decision rule enforced in Equation (29) could be rewritten as given in Equation (31).

$$_{MD} = \arg Max_i \left[\frac{1}{\delta_i}\right] \tag{31}$$

Above decision rule helps to classify the instance according to its distance with class centroids available in feature space. This classifier model seems to be more simple and computationally efficient in producing the result with multi-class probabilities. At the time of classification, the features may contribute unequally and deform the distance function due to the availability of noisy and irrelevant features. Therefore, feature weight is embedded with the minimum distance classifier model to enhance the performance and interoperability by moderating the role of less-relevant features into the distance function as expressed by Equation (32).

$$\delta_i^2 = \sum_{i=1}^{d} \mathcal{W}_i \left(\mathcal{Y}_i - m_i\right)^2 \tag{32}$$

Let $\mathcal{W}_i$ be the weight factor of i^{th} feature with constraints such as $\mathcal{W}_i \geq 0$ and $\sum_{i=1}^{d} \mathcal{W}_i = 1$. This modified distance measure applied in Equation (31) gives way to a feature-weighted minimum distance classifier model. So, a normalised score is used for the feature-weight distance as a confidence measure. Moreover, the proposed classifier can easily handle the higher dimensional data by improving the role of dominant features and minimising the unbalanced effect of weaker features. Initially, the nearest class centroid is the only parameter explored by the proposed classifier during the training phase. Then, the distance measurement from the testing sample to the class centroid is

obtained with the appropriate class label and self-belief during the testing phase.

3. Experimental evaluations

To evaluate the performance of the proposed feature-weighted minimum distance, classifier model is compared against the existing classifiers. Moreover, the KPCA feature selection method is applied to improve the robustness of the proposed VIPDIS. In order to effectively measure the performance of the healthcare systems, a benchmarking dataset is explored from the recent literature study (Li et al., 2018). It consists of various classes of walking persons such as normal, hemiplegia, and Parkinson summarised with characteristics and classification accuracy as illustrated in Table 1. In this dataset, 14 different persons walking sequences were observed along the line by facing the camera at ordinary speed. During experimentation, each person five autonomous walking sequences are captured and resulting in 5×14 dataset. Here, hemiplegia has significant consequences on body functionality pertaining to its severity levels and types. In the case of Parkinson's disease, fundamental clinical symptoms are observed such as rigidity, rest tremor, bradykinesia, and disorder in gait balance. Then, the impact of time window size is enforced on the results as shown in Table 2.

More evident from Table 2, the proposed feature-weighted minimum distance classifier model provides very good classification accuracy by varying the window size range of 5, 10, 15, and 20. Further, the walking cycle and full gait sequence are also considered during the experimentation. Here, a more optimal result is obtained during the experimentation with the window size of 10. The performance of various classifier models is measured by applying the feature selection methods such as correlation-based feature selection (CFS), PCA, and, KPCA. Corresponding results are observed in terms of prediction time (seconds) and prediction accuracy (percentage) as given in Table 3. Clearer from observation, the proposed feature-weighted minimum distance classifier model achieves better prediction time and accuracy against the existing classifier models with PCA and CFS feature selection approaches. Table 1 gives the general classification information of classes such as normal, hemiplegic, and Parkinson. The actual prediction time and prediction accuracy of the classifier is given in the Table 3, where the proposed feature-weighted minimum distance classifier model is compared against the existing support vector machine classifier and ensemble learning classifier models. To get better descriptive analysis on the model, the comparative analysis is shown in the Figure 2 and Figure 3.

As per the experimental observation, the proposed classifier provides an average improvement of 7.83%, 4.23%, and 2.55% prediction accuracy over the existing classifiers with respect to KPCA, CFS and PCA approaches, respectively. Similarly, the proposed classifier provides an average improvement of 10.69%, 8.94%, and 6.34% prediction time over the existing classifiers with respect to KPCA, CFS, and PCA, respectively. These improvements in prediction time and accuracy were achieved due to the incorporation of feature-weighted minimum distance classifier model in the proposed VIPDIS. In the future, the research study can be enhanced to improve the gait pattern recognition rate by applying the two-dimensional image features. Sometimes, the motion data are very difficult to acquire during real-time experimentation because of occlusions and the quick movement of humans. This scenario could completely disappear some important and even complete frames of the skeleton. Also, the low resolution of data captured during gait analysis may be more challenging owing to hampers illustration and subtle motion recognition. Significant improvement can be made in the gait pattern recognition by using the edge-fog-cloud integrated healthcare platform (Rajavel et al., 2022). Moreover, the selection of optimal healthcare services offered from the different providers can be done through

Table 1. Classification accuracy.

Classes	Age Differences (Years)	Worst Case Accuracy (%)	Best Case Accuracy (%)
Normal	46–75 years	71.1	94.4
Hemiplegic	50–83 years	67.8	92.2
Parkinson	60–85 years	61.1	90.0

Table 2. Stride results of acceleration data.

Window Size	VIPDIS Classification Accuracy (%)		
	Support Vector Machine Classifier	Ensemble Learning Classifier	Proposed Feature-weighted Minimum Distance Classifier
5	75.6	77.2	79.6
10	86.8	87.5	89.7
15	85.4	88.3	90.2
20	84.8	86.7	89.5
Walk Cycle	82.3	84.3	89.3
Full Sequence	80.4	81.6	87.2

Table 3. Performance of various classifier models during entire gait sequence.

Classifier Models	Feature Extraction Technique	Prediction Time (Seconds)	Prediction Accuracy (%)
Support Vector Machine Classifier	KPCA	78.56	85.3
	CFS	80.23	83.5
	PCA	81.33	82.3
Ensemble Learning Classifier	KPCA	80.56	86.4
	CFS	85.34	85.6
	PCA	87.45	83.7
Feature-Weighted Minimum Distance Classifier	KPCA	68.89	93.6
	CFS	70.45	90.4
	PCA	72.76	88.9

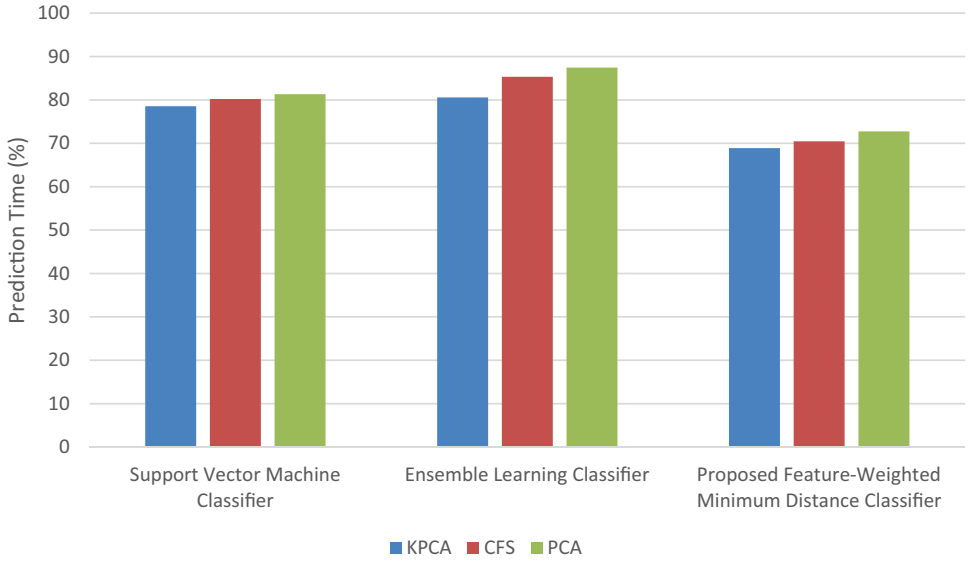

Figure 2. Performance of classifier models with respect to prediction time.

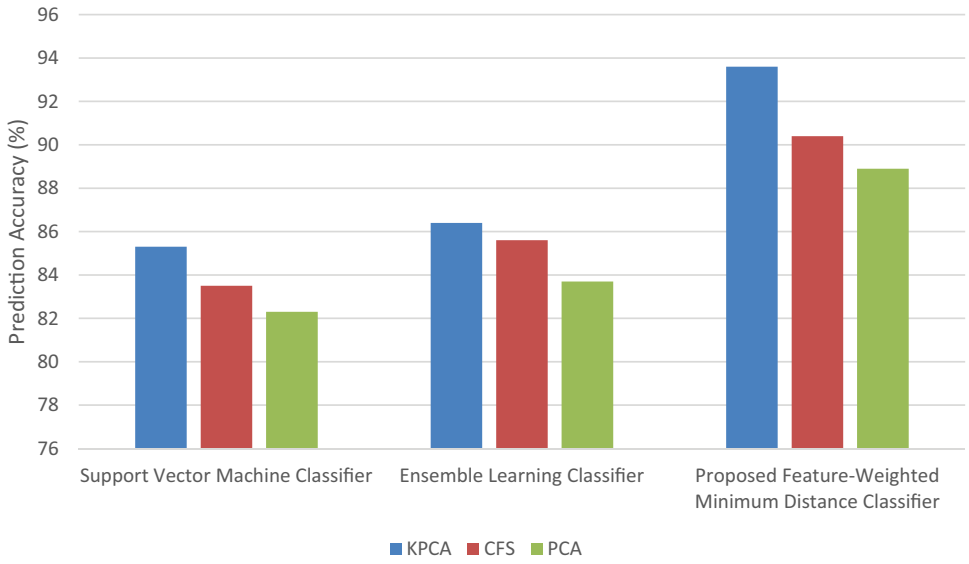

Figure 3. Performance of classifier models with respect to prediction accuracy.

an effective negotiation framework (Kamran et al., 2021; Rajavel & Thangarathanam, 2016).

4. Conclusion and future works

In this research study, the problem of identifying Parkinson disease using the vision-based gait feature extraction is captured by the raspberry pi-3 camera module. Although gait analysis plays an important role in the real-time prediction and diagnosis of Parkinson's disease, there are a limited number of vision-based methodologies available in the current research studies. The proposed research enhances the performance of the healthcare system by applying the KPCA-based feature extraction and a feature-weighted minimum distance classifier model in the VIPDIS. It uses the image sequence of silhouettes captured during the human walking state and extracts the appropriate features to support the prediction and diagnosis. To validate the performance of VIPDIS, the comparative analysis of proposed KPCA-based feature extraction is made against the existing CFS and PCA feature extraction approaches with respect to prediction time and accuracy. Moreover, the performance of VIPDIS is measured over various models such as support vector machine, ensemble learning, and feature-weighted minimum distance classifiers. As a result, the proposed classifier model with KPCA-based feature extraction obtains 10.69% and 7.83% improvements on prediction time and accuracy while comparing to the existing classifier models.

In the future, the performance can be improved through the enforcement of kinetic sensor-based gait analysis during the experimentation.

Disclosure statement

No potential conflict of interest was reported by the author(s).

Data availability statement

The dataset exploited in this research study is available online from "Classification of gait anomalies from kinect", The Visual Computer, Vol. 34, pp. 229–241, 2018. https://doi.org/10.1007/s00371-016-1330-0

References

Bandini, A., Orlandi, S., Escalante, H. J., Giovannelli, F., Cincotta, M., Reyes-Garcia, C. A., Vanni, P., Zaccara, G., & Manfredi, C. (2017). Analysis of facial expressions in Parkinson's disease through video-based automatic methods. *Journal of Neuroscience Methods*, *281*, 7–20. http://dx.doi.org/doi:10.1016/j.jneumeth.2017.02.006

Benmalek, E., Elmhamdi, J., & Jilbab, A. (2018). Multiclass classification of Parkinson's disease using cepstral analysis. *International Journal of Speech Technology*, *21*(1), 39–49. https://doi.org/10.1007/s10772-017-9485-2

Buongiorno, D., Bortone, I., Cascarano, G. D., Trotta, G. F., Brunetti, A., & Bevilacqua, V. (2019). A low-cost vision system based on the analysis of motor features for recognition and severity rating of Parkinson's disease. *BMC Medical Informatics and Decision Making*, *19*(Suppl 9), 243. https://doi.org/10.1186/s12911-019-0987-5

Cancela, J., Fico, G., & Waldmeyer, M. T. A. (2015). Using the ieanalytic hrarchy process (AHP) to understand the most important factors to design and evaluate a telehealth system for Parkinson's disease. *BMC Medical Informatics and Decision Making*, *153*(Suppl 3), S7. https://doi.org/10.1186/1472-6947-15-S3-S7

Debû, B., Godeiro, C. D. O., Lino, J. C., & Moro, E. (2018). Managing gait, balance, and posture in Parkinson's disease. *Current Neurology and Neuroscience Reports*, *18*(23), 1–12. https://doi.org/10.1007/s11910-018-0828-4

Diallo, O., Rodrigues, J. J. P. C., Sene, M., & Niu, J. (2014). Real-time query processing optimization for cloud-based wireless body area networks. *Information Sciences*, *284*, 84–94. http://dx.doi.org/10.1016/j.ins.2014.03.081

Fisher, J. M., Hammerla, N. Y., Ploetz, T., Andras, P., Rochester, L., & Walker, R. W. (2016). Unsupervised home monitoring of Parkinson's disease motor symptoms using body-worn accelerometers. *Parkinsonism and Related Disorders*, *33*, 44–50. http://dx.doi.org/10.1016/j.parkreldis.2016.09.009

Gómeza, P., Mekyska, J., Gómez, A., Palacios, D., Rodellar, V., & Álvarez, A. (2019). Characterization of Parkinson's disease dysarthria in terms of speecharticulation kinematics. *Biomedical Signal Processing and Control*, *52*, 312–320. https://doi.org/10.1016/j.bspc.2019.04.029

Hellqvist, C., & Berterö, C. (2015). Support supplied by Parkinson's disease specialist nurses to Parkinson's disease patients and their spouses. *Applied Nursing Research*, *28*(2), 86–91. http://dx.doi.org/10.1016/j.apnr.2014.12.008

Hussain, A., Wenbi, R., Silva, A. L. D., Nadher, M., & Mudhish, M. (2015). Health and emergency-care platform for the elderly and disabled people in the smart city. *The Journal of Systems and Software*, *110*, 253–263. http://dx.doi.org/10.1016/j.jss.2015.08.041

Kamran, I., Naz, S., Razzak, I., & Imran, M. (2021). Handwriting dynamics assessment using deep neural network for early identification of Parkinson's disease. *Future Generation Computer Systems*, *117*, 234–244. https://doi.org/10.1016/j.future.2020.11.020

Karan, B., Sahu, S. S., Orozco-Arroyave, J. R., & Mahto, K. (2020). Hilbert spectrum analysis for automatic detection and evaluation ofParkinson's speech. *Biomedical Signal Processing and Control*, *61*, 102050. https://doi.org/10.1016/j.bspc.2020.102050

Khlebtovsky, A., Djaldetti, R., Rodity, Y., Keret, O., Tsvetov, G., Slutzcki-Shraga, I., & Benninger, F. (2017). Progression of postural changes in Parkinson's disease: Quantitative assessment. *Journal of Neurology*, *264*(4), 675–683. https://doi.org/10.1007/s00415-017-8402-6

Kim, Y., & Lee, S. (2014). Energy-efficient wireless hospital sensor networking for remote patient monitoring. *Information Sciences*, *282*, 332–349. http://dx.doi.org/10.1016/j.ins.2014.05.056

Kruger, R., Klucken, J., Weiss, D., Tonges, L., Kolber, P., Unterecker, S., Lorrain, M., Baas, H., Muller, T., & Rieder, P. (2017). Classification of advanced stages of Parkinson's disease: Translation into stratified treatments. *Journal of Neural Transmission*, *124*(8), 1015–1027. https://dx.doi.org/10.1007%2Fs00702-017-1707-x

Li, Q., Wang, Y., Sharf, A., Cao, Y., Tu, C., Chen, B., & Yu, S. (2018). Classification of gait anomalies from kinect. *The Visual Computer*, *34*(2), 229–241. https://doi.org/10.1007/s00371-016-1330-0

Machado, I. P., Gomes, A. L., Gamboa, H., Paixão, V., & Costa, R. M. (2015). Human activity data discovery from triaxial accelerometer sensor: Non-supervised learning sensitivity to feature extraction parametrization. *Information Processing and Management*, *51*(2), 204–214. http://dx.doi.org/10.1016/j.ipm.2014.07.008

Mamun, K. A. A., Alhussein, M., Sailunaz, K., & Islam, M. S. (2017). Cloud based framework for Parkinson's disease diagnosis and monitoring system for remote healthcare applications. *Future Generation Computer Systems*, *66*, 36–47. http://dx.doi.org/10.1016/j.future.2015.11.010

Nancy Noella, R. S., Gupta, D., & Priyadarshini, J. (2019). Diagnosis of Parkinson's disease using Gait dynamics and images. *Procedia Computer Science*, *165*, 428–434. https://doi.org/10.1016/j.procs.2020.01.002

Ortells, J., Herrero-Ezquerro, M. T., & Mollineda, R. A. (2018). Vision-based gait impairment analysis for aided diagnosis. *Medical & Biological Engineering & Computing*, *56*(9), 1553–1564. https://doi.org/10.1007/s11517-018-1795-2

Pourghayoomi, E., Behzadipour, S., Ramezani, M., Joghataei, M. T., & Shahidi, G. A. (2020). A new postural stability-indicator to predict the level of fear of falling in Parkinson's disease patients. *BioMedical Engineering OnLine*, *19*(64), 1–18.

Rajavel, R., Ravichandran, S. K., Harimoorthy, K., Nagappan, P., & Gobichettipalayam, K. R. (2022). IoT-based smart healthcare video surveillance system using edge computing. *Journal of Ambient Intelligence and Humanized Computing*, *13*(6), 3195–3207. https://doi.org/10.1007/s12652-021-03157-1

Rajavel, R., & Thangarathanam, M. (2016). Adaptive probabilistic behavioural learning system for the effective behavioural decision in cloud trading negotiation market. *Future Generation Computer Systems*, *58*, 29–41. https://doi.org/10.1016/j.future.2015.12.007

Rajavel, R., & Thangarathanam, M. (2021). Agent-based automated dynamic SLA negotiation framework in the cloud using the stochastic optimization approach. *Applied Soft Computing*, *101*, 107040. https://doi.org/10.1016/j.asoc.2020.107040

Rodriguez-Martin, D., Samà, A., Perez-Lopez, C., Català, A., Cabestany, J., & Rodriguez-Molinero, A. (2013). SVM-based posture identification with a single waist-located triaxial accelerometer. *Expert Systems with Applications*, *40*(18), 7203–7211.

Sonawane, B., & Sharma, P. (2021). Review of automated emotion-based quantification of facial expression in Parkinson's patients. *The Visual Computer*, *37* (5), 1151–1167. https://doi.org/10.1007/s00371-020-01859-9

Vermilyea, S. C., & Emborg, M. E. (2018). The role of nonhuman primate models in the development of cell based therapies for Parkinson's disease. *Journal of Neural Transmission*, *125*(3), 365–384. https://doi.org/10.1007/s00702-017-1708-9

Waldthaler, J., Krüger-Zechlin, C., Stock, L., Deeb, Z., & Timmermann, L. (2019). New insights into facial emotion recognition in Parkinson's disease with and without mild cognitive impairment from visual scanning patterns. *Clinical Parkinsonism & Related Disorders*, *1*, 102–108. http://dx.doi.org/10.1016/j.prdoa.2019.11.003

Xu, S., & Pan, Z. (2020). A novel ensemble of random forest for assisting diagnosis of Parkinson's Disease on small handwritten dynamics dataset. *International Journal of Medical Informatics*, *144*, 104283. https://doi.org/10.1016/j.ijmedinf.2020.104283